Powder Technology 286 (2015) 716–721

Contents lists available at ScienceDirect

Powder Technology

journal homepage: www.elsevier.com/locate/powtec

Effect of Al addition on the microstructures and compression properties of (TiC_xN_y–TiB_2)/Ni composites fabricated by combustion synthesis and hot press

Feng Qiu [a,c], Rui Zuo [a], Shi-Li Shu [b], Ya-Wei Wang [a], Qi-Chuan Jiang [a,*]

[a] Key Laboratory of Automobile Materials, Ministry of Education, Department of Materials Science and Engineering, Jilin University, No. 5988 Renmin Street, Changchun 130025, People's Republic of China
[b] State Key Laboratory of Luminescence and Applications, Changchun Institute of Optics, Fine Mechanics and Physics, Chinese Academy of Sciences, 130012 Changchun, People's Republic of China
[c] Department of Mechanical Engineering, Oakland University, Rochester, MI 48309, United States

ARTICLE INFO

Article history:
Received 28 May 2015
Received in revised form 19 August 2015
Accepted 9 September 2015
Available online 11 September 2015

Keywords:
Ceramics
Composites
Powder metallurgy

ABSTRACT

The 70 wt.% (TiC_xN_y–TiB_2)/Ni composites were fabricated successfully by the combustion synthesis and hot press consolidation of the Ni–Ti–Al–B_4C–BN powder mixtures. The addition of Al to Ni–Ti–B_4C–BN system significantly decreased the ignition difficulty of combustion synthesis, and improved the compression properties of (TiC_xN_y–TiB_2)/Ni composites. The final products mainly consist of Ni, TiC_xN_y and TiB_2, and the ceramic particles distribute uniformly in the composites. With increasing Al content from 0 to 8 wt.%, the average sizes of the TiC_xN_y and TiB_2 particles decrease a little, while the hardness and the compression strength increase firstly and then decrease, and the fracture strain increases. The composite with optimal 5 wt.% Al possesses the best comprehensive properties: the highest hardness (1794 Hv), the superior compression strength (3.76 GPa), and the fracture strain (4.2%), resulting in an overall increase by ~15%, ~28%, and ~45%, compared with these of the composite without the Al addition, respectively.

1. Introduction

Compared with the WC–Co cemented carbides, TiC_xN_y ($x + y \le 1$) and TiB_2 ceramics possess better properties, such as higher hardness, good wear resistance, superior cutting performance, and better oxidation resistance [1–7], and thus, they have been promising candidates for cutting tool materials. However, since the wettability of Ni binder on the Ti(C_xN_y) and TiB_2 is worse than that of Co binder on the WC, Ti(C_xN_y)/Ni and TiB_2/Ni composites possess the less toughness, contributing to their limited application [8,9]. Lately, some researchers reported that some elements, such as Mo, could improve the wettability between ceramics and metallic binder Ni, refine the ceramic particles and enhance the compression properties. Parikh and Humenik reported that the contact angle of Ni on TiC in vacuum decreased with the addition of 10 wt.% Mo [10,11]. LaSalvia's results showed that the addition of Mo resulted in a decline in the number of interphase debinding and binder micro-cracking [12]. Due to the low specific gravity, and strong chemical activity of Al with Ni, it is reasonable that Al has the potential to enhance the mechanical properties of the composites. Till now, the effect of Al was still rarely reported.

Combustion synthesis has many advantages, such as dispersing the ceramic uniformly, clean particle-matrix interface and simplicity of experimental set-up due to lower reaction temperature [13–15]. In order to improve the final density of the composites, an additional mechanical pressure was applied, which is commonly defined as combustion synthesis and hot press consolidation [16].

In this work, the (TiC_xN_y–TiB_2)/Ni composites with different contents of Al were fabricated by the method of combustion synthesis and hot press consolidation at a relatively low processing temperature (~1073 K). Meanwhile, the effects of the Al content on the relative density, hardness, microstructures and compression properties of the (TiC_xN_y–TiB_2)/Ni composites were investigated in detail. The addition of Al can improve the comprehensive properties of the (TiC_xN_y–TiB_2)/Ni composites. It will offer some guidance to the fabrication, investigation and application of the Ni matrix composites, even more to the other metal matrix composites.

2. Experimental

The raw materials used were commercial powders of Ni (99.5% purity, ~58 μm), Al (99% purity, ~75 μm), Ti (99% purity, ~25 μm), BN (99% purity, ~3.0 μm) and B_4C (99% purity, ~3.5 μm). The nominal content of the ceramic particles fabricated in the composites was 70 wt.%, and the mole ratio of Ti:BN:B_4C was fixed as 9:2:2

* Corresponding authors.
E-mail address: qiufeng@jlu.edu.cn (F. Qiu).

http://dx.doi.org/10.1016/j.powtec.2015.09.016
0032-5910/

corresponding to the reaction Eq. (1). The content of Al increases from 0 to 8 wt.%.

$$9\,Ti + 2\,BN + 2\,B_4C \rightarrow 4\,Ti(C_{0.5}N_{0.5}) + 5\,TiB_2 \quad (1)$$

The mixed powders were dry-mixed in a stainless-steel container with stainless-steel balls at a low speed (50 rpm) for 8 h. Then, the powders were uniaxially cold pressed in the stainless steel dies. The powder mixtures of the Ni–Ti–BN–B_4C and the Ni–8Al–Ti–BN–B_4C powders were performed for DTA (TA SDT-Q600, USA) experiment in order to analyze the phase transitions in the Ni–Ti–BN–B_4C and the Ni–8Al–Ti–BN–B_4C powders. A small amount of the reactants weighing about 50 ± 5 mg were held in an alumina crucible and heated to 1230 °C at a heating rate of 40 °C/min, and some interrupted runs were performed in order to obtain the intermediate reaction products.

The prepared cylindrical green compact with 28 mm in diameter was placed in a set of graphite dies, which was put into the self-made vacuum thermal explosion furnace (shown in Fig. 1). The heating rate of the furnace was about 0.5 K/s in a vacuum atmosphere. Once the composite synthesis reaction was ignited, the compact was quickly pressed just when it was hot and soft. The pressure (~40 MPa) was maintained for 30 s and then sample was cooled down to the room temperature.

The combustion temperature experiments were conducted in a self-made vacuum vessel in an Ar atmosphere. During the reaction process, the temperature in the position about 3 mm beneath the center of the compact top surface was measured by W5-Re26 thermocouples, W5-Re26 is the index number of the thermocouple, and the signals were recorded and processed by a data acquisition system using an acquisition speed of 50 ms per point.

The phase constituent of DTA products and the bulk samples were investigated by XRD (D/Max 2500PC Rigaku, Japan) using Cu Kα radiation. The microstructure and the fracture surfaces were examined by a SEM (Evo18, Carl Zeiss, Germany) equipped with an energy-dispersive spectrometer (Link-ISIS, Oxford, Britain). The density was determined by the method of Archimedes' principle. Microhardness of the composites was measured by a Vickers hardness tester (1600-5122VD Micromet 5104, USA) using a static load of 10 N and a dwell time of 15 s. The uniaxial compression tests were carried out under servo-hydraulic material testing system (MTS, MTS 810, USA) at a strain rate of $1 \times 10^{-4}\ s^{-1}$.

3. Results and discussion

3.1. Phase identification and microstructures

Fig. 2 shows the DTA curves for the Ni–Ti–BN–B_4C and the Ni–8Al–Ti–BN–B_4C powders. In the Ni–Ti–BN–B_4C system, a significant exothermic peak starts at near 1069 °C, and two exothermic peaks follow immediately at 1130 °C and 1174 °C. In the Ni–8Al–Ti–BN–B_4C system, an endothermic peak appears at temperatures close to 660 °C, corresponding to the melting of Al, from 730 °C to start an obvious exothermic peak, continue to 830 °C. It shows that there will be a long time exothermic reaction during this stage, and the reaction is not severe. When the temperature increased to 1070 °C, it appears a weak endothermic peak, then, other two strong exothermic peaks appeared at 1085 °C and 1134 °C, respectively.

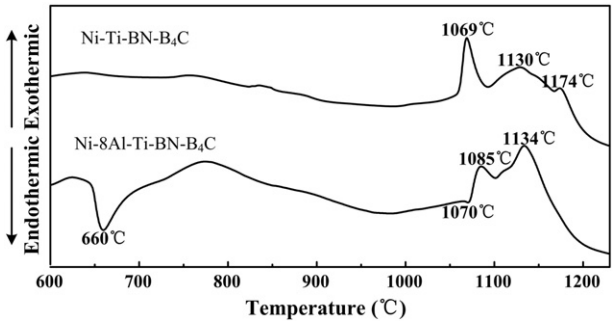

Fig. 2. DTA curves of the Ni–Al–Ti–BN–B_4C reactant mixture with 0 wt.% and 8 wt.% Al at the heating rate of 40 °C/min to 1230 °C in the condition of flowing Ar.

In order to develop an understanding of the phase transitions in the Ni–Ti–BN–B_4C and Ni–8Al–Ti–BN–B_4C systems, experiments quenched at about 1050 °C, 1085 °C, 1160 °C and 1180 °C were carried out in the Ni–Ti–BN–B_4C mixtures, and experiments quenched at about 700 °C, 1000 °C, 1100 °C and 1150 °C were carried out in the Ni–8Al–Ti–BN–B_4C mixtures. Fig. 3 shows the XRD analysis results of the quenched sample in the Ni–Ti–BN–B_4C system. As indicated, the phase constituents of sample quenched at different temperatures show a remarkable change. When the products heated below 1050 °C, the Ni, Ni_3B, Ni_3Ti and $TiN_{0.3}$ phases were detected, indicating the occurrence of reactions between Ni and Ti, Ti and BN, and Ni and BN. It suggested that some solid-state diffusion reactions had occurred among these reactants and the occurrence of the reaction between Ti and BN is somewhat easier than the others. When the products heated to 1085 °C, the Ni, Ni_3B, Ni_3Ti and $TiN_{0.3}$ phases were detected [see Fig. 3(b)], and TiC_xN_y and

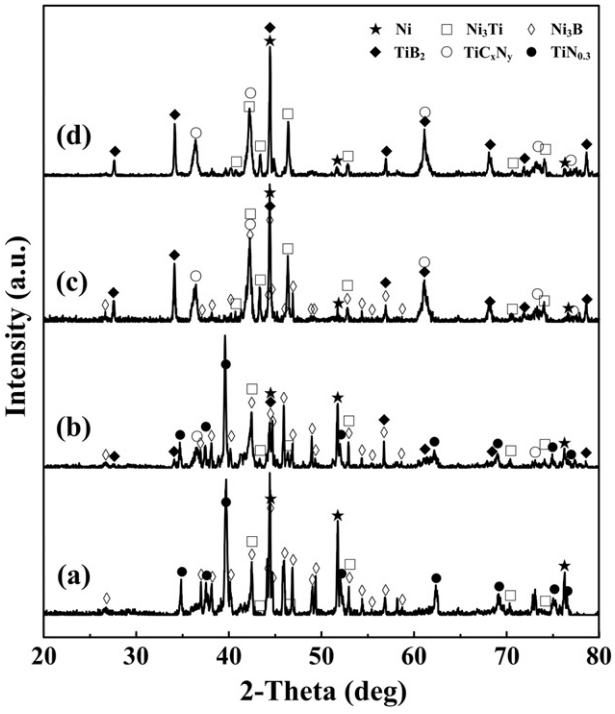

Fig. 3. X-ray diffraction patterns of the Ni–Ti–BN–B_4C system quenched from different temperatures: (a) 1050 °C, (b) 1085 °C, (c) 1160 °C and (d) 1180 °C, respectively.

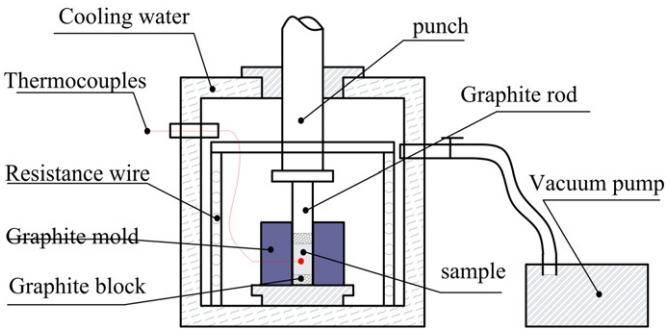

Fig. 1. Schematic of the equipment for the combustion synthesis and hot press consolidation.

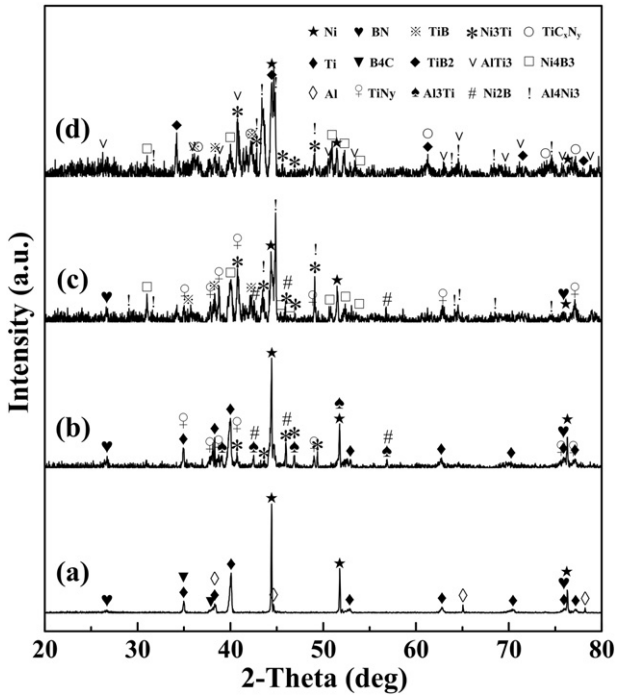

Fig. 4. X-ray diffraction patterns of the Ni–8Al–Ti–BN–B_4C system quenched from different temperatures: (a) 700 °C, (b) 1000 °C, (c) 1100 °C and (d) 1150 °C, respectively.

some TiB_2 were detected. It indicated that the exothermic event at 1069 °C was caused by the formation of TiC_xN_y. From Fig. 3(c) can be seen, after heating the Ni–Ti–BN–B_4C mixture to 1160 °C, a mass of Ni, Ni_3Ti, TiC_xN_y, TiB_2 and Ni_3B phase were detected in the quenched products, while the $TiN_{0.3}$ phase disappeared. It indicated that the exothermic event at 1130 °C was also caused by the formation of TiC_xN_y and TiB_2. Up to the temperature of 1180 °C, the diffraction peaks of Ni, Ni_3Ti, TiC_xN_y and TiB_2 phases were detected in the quenched products, and Ni_3B phases disappeared. It meant that the reaction was completed at 1180 °C, and a large number of the final product of reaction was generated, such as TiC_xN_y and TiB_2. At 1174 °C, the strong exothermic peak was caused by the TiB_2 formation.

The XRD patterns of products were shown in Figs. 4(a–d). As shown in Fig. 4(a), there is no reaction that occurred before 700 °C in the Ni–8Al–Ti–BN–B_4C system. When the products heated to 1000 °C, the Ni_3Ti, TiN_y, Al_3Ti, and Ni_2B phases were detected, indicating the

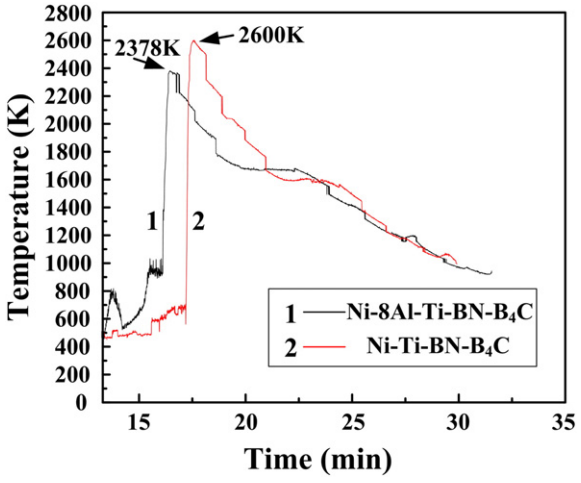

Fig. 5. The typical temperature profiles for the Ni–Ti–B_4C–BN and Ni–Al–Ti–B_4C–BN compacts in the thermal explosion reactions.

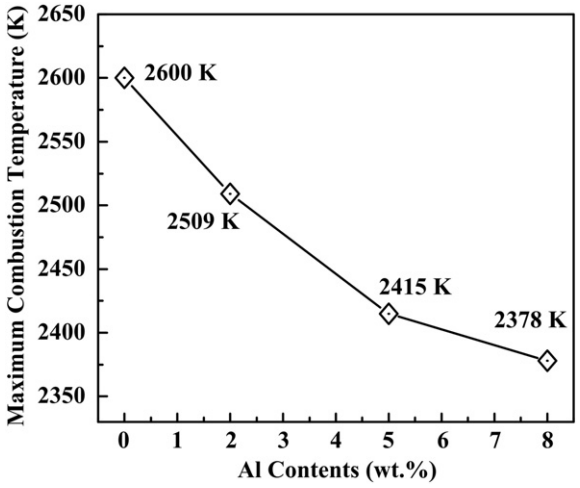

Fig. 6. Variation of the maximum combustion temperature in the Ni–Al–Ti–B_4C–BN system with different Al contents.

occurrence of reactions between Ni and Ti, Al and Ti, Ti and BN, Ni and BN and the presence of the liquid phase promotes the formation of these compounds. From Fig. 4(c) can be seen, at 1100 °C, Ti phase disappears, and the TiB and Ni_4B_3 phases appear. In addition, a large number of intermetallic compounds, such as $AlTi_3$, Al_4Ni_3 and Ni_3Ti phases, begin to appear. It shows that in Fig. 2, the endothermic peak at 1070 °C is due to the formation of large amounts of liquid phase, and the phase of liquid also promotes the reaction process. The exothermic peak at 1085 °C mainly related to the formation of TiB. This is because only TiB can release such intense heat (as shown in Eq. (2)).

$$Ti + B \rightarrow TiB \qquad \Delta H = -160.25 \quad kJ/mol \tag{2}$$

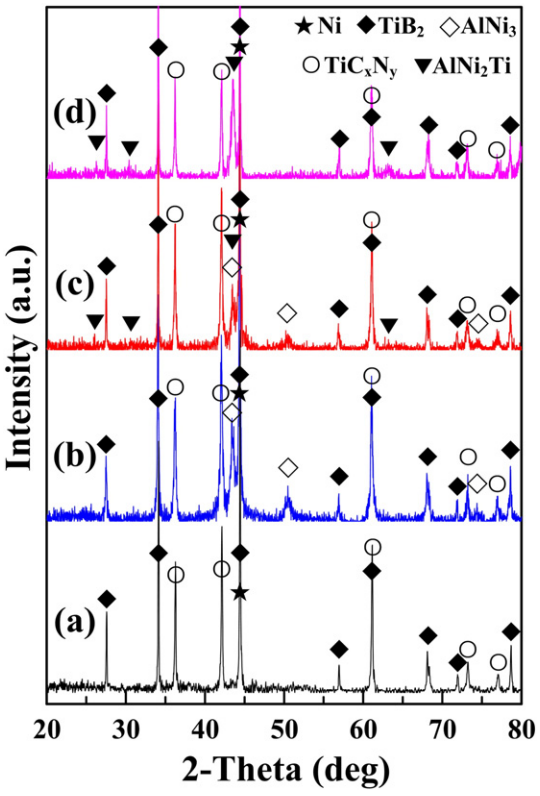

Fig. 7. X-ray diffraction patterns for the composites with different Al contents: (a) 0, (b) 2, (c) 5 and (d) 8 wt.%, respectively.

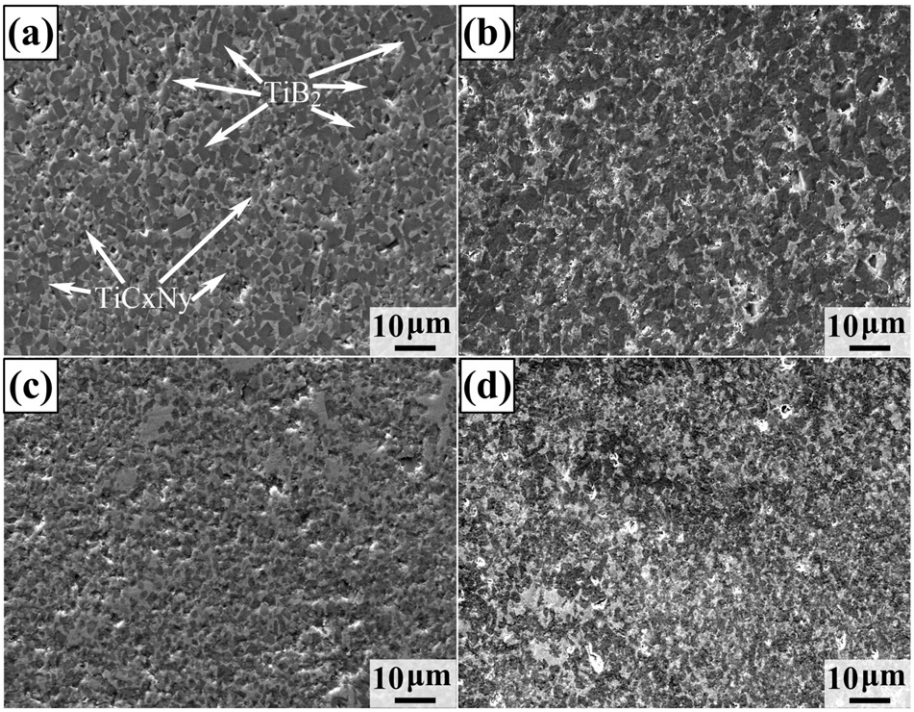

Fig. 8. Microstructures of the (TiC_xN_y–TiB_2)/Ni composites with different Al contents: (a) 0, (b) 2, (c) 5 and (d) 8 wt.%, respectively.

Up to the temperature of 1150 °C, the diffraction peaks of TiC_xN_y and TiB_2 phases are detected in the quenched products, and the TiN_y, Ni_2B and BN phases are disappeared. It means that the reaction is completed at 1150 °C, and a large number of the final product of reaction is generated, such as TiC_xN_y and TiB_2. At 1134 °C, the wide strong exothermic peak is due to the formation of TiC_xN_y and TiB_2. TiC_xN_y and TiB_2 formation. Compared with Ni–Ti–BN–B_4C system, a large number of liquid phase appear in the Ni–8Al–Ti–BN–B_4C system at 1070 °C, and the complete reaction temperature is reduced from 1174 °C to 1134 °C. It could decrease the maximum combustion temperature of the Ni–Al–Ti–B_4C–BN system.

Fig. 5 shows the typical temperature profiles for the Ni–Ti–B_4C–BN and Ni–Al–Ti–B_4C–BN compacts in the thermal explosion reactions. Fig. 6 shows the variation of the maximum combustion temperature in Ni–Al–Ti–B_4C–BN systems with different Al contents. It is observed that the maximum combustion temperature of the Ni–Al–Ti–B_4C–BN system decreases sharply from 2600 K to 2378 K with increasing Al content from 0 to 8 wt.%. The melting point of Al is about 660 °C and the temperature will reach 800 °C during the heating process before the thermal explosion reaction, so Al has already melted before the reaction. With Al addition, the liquid phase appears at lower temperature, the addition of Al can promote the reaction of Al reacting with other elements, and the maximum combustion temperature is reduced.

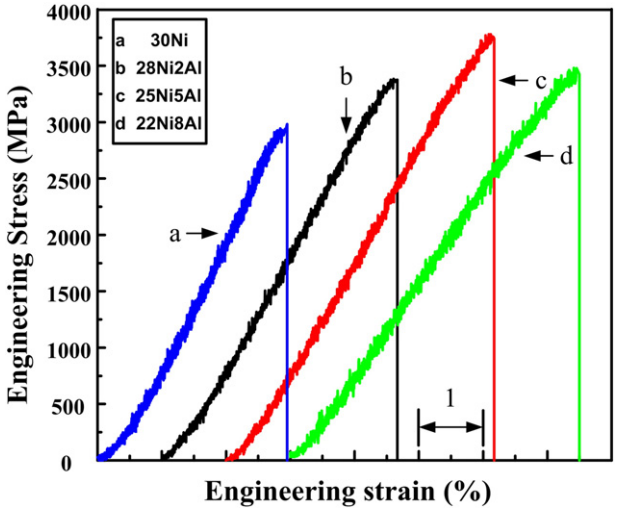

Fig. 9. Compression engineering stress–strain curves of the (TiC_xN_y–TiB_2)/Ni composites with different Al contents.

The reaction mechanism in the thermal explosion reaction of the Ni–Al–Ti–B_4C–BN compacts could be described as follows: The explosion reaction in the Ni–Al–Ti–B_4C–BN systems starts with the formation of Ni_3Ti, Al_3Ti, TiN_y and Ni_2B phases from the reactions between Ni and Ti, Al and Ti, Ti and BN, and Ni and BN, respectively. With the addition of Al, the liquid phase appears at a lower temperature, the addition of Al can promote the reaction of Al reacting with other elements. Subsequently, the Ni–Al–Ti liquid is formed from the melting of the Ni–Al–Ti phase. The Ni–Al–Ti liquid spreads over the BN, B_4C and the remaining Ti particles. Subsequently, the carbon, boron and nitrogen atoms from the bulk B_4C and BN continuously diffuse into the liquid phase to form Ni–Al–Ti–B–C–N liquid. TiB generated and precipitates from the Ni–Al–Ti–B–C–N liquid. The heat generated from these reactions promotes the further dissolution of the C, B and N atoms in the Ni–Al–Ti liquid to form the Ni–Al–Ti–B–C–N liquid. As the B, N and C atoms in the liquid become sufficiently supersaturated, a plenty of TiB_2 and TiC_xN_y grains begin to precipitate.

Table 1
Density and relative density of the cylindrical powder compacts.

Samples	Density (g/cm^3)	Relative density (%)
30 wt.% Ni + 0 wt.% Al	3.474 ± 0.026	66.3 ± 0.5
28 wt.% Ni + 2 wt.% Al	3.422 ± 0.031	65.8 ± 0.6
25 wt.% Ni + 5 wt.% Al	3.341 ± 0.032	65.9 ± 0.6
22 wt.% Ni + 8 wt.% Al	3.338 ± 0.036	66.1 ± 0.7

Table 2
Room-temperature compression properties, measured density and microhardness of the 70 wt.% (TiC_xN_y–TiB_2)/Ni composites with different Al contents.

Samples	Measured density (g/cm^3)	σ_{UCS} (GPa)	ε_f (%)	Hv
30 wt.% Ni + 0 wt.% Al	5.24 ± 0.08	2.94 ± 0.11	2.9 ± 0.2	1561 ± 36
28 wt.% Ni + 2 wt.% Al	5.20 ± 0.08	3.36 ± 0.09	3.7 ± 0.2	1691 ± 45
25 wt.% Ni + 5 wt.% Al	5.07 ± 0.07	3.76 ± 0.15	4.2 ± 0.3	1794 ± 39
22 wt.% Ni + 8 wt.% Al	5.05 ± 0.06	3.47 ± 0.12	4.5 ± 0.2	1513 ± 28

Fig. 7 shows XRD patterns for the 70 vol.% (TiC_xN_y–TiB_2)/Ni composites with 0, 2, 5 and 8 wt.% Al addition. Only the Ni, TiB_2 and TiC_xN_y phases are detected in the absence of Al. The addition of 2 wt.% Al results in the formation of $AlNi_3$. Further increasing the Al content to 5 wt.% formed $AlNi_2Ti$, and simultaneously weaken the (200) and (220) diffraction peak of $AlNi_3$ phase. When the content of Al is 8 wt.%, only Ni, TiB_2, TiC_xN_y and $AlNi_2Ti$ are detected in the composites. Fig. 8 shows the SEM images of the 70 vol.% (TiC_xN_y–TiB_2)/Ni composites with 0, 2, 5 and 8 wt.% Al addition. The composites are dense. The synthesized TiC_xN_y particles are in the shape of near-spherical or spherical shape, while the TiB_2 particles are in the shape of rectangular or hexagonal shape. They are all distributed uniformly in the Ni matrix, and the sizes of the ceramic particles decrease from about 4 μm to less than 2 μm with the addition of Al. The decreasing of the ceramic particle sizes might be attributed to the decrease of the maximum combustion temperature. The maximum combustion temperature of the Ni–Al–Ti–B_4C–BN system decreases sharply from 2600 K to 2378 K with increasing Al content from 0 to 8 wt.%. With Al addition, a large number of liquid phase appear at lower temperature, the addition of Al can promote the reaction of Al reacting with other elements, and the maximum combustion temperature are reduced. Furthermore, the addition of Al increased the density due to the binder effect.

3.2. Compression properties

Fig. 9 shows the compression engineering stress–strain curves of the (TiC_xN_y–TiB_2)/Ni composites, and the compression properties and hardness are given in Table 2. With the increase of Al content from 0 to 5 wt.%, the ultimate compression strength (σ_{UCS}), fracture strain (ε_f), and microhardness (Hv) of the composites increase from 2.94 GPa, 2.9%, and 1561 Hv to 3.76 GPa, 4.2% and 1794 Hv, respectively. Further increasing Al content to 8 wt.%, σ_{UCS}, and Hv decrease, and ε_f increases a little. The (TiC_xN_y–TiB_2)/Ni composites with 5 wt.% Al possess the best comprehensive properties: the highest Hv (1794 Hv), the superior σ_{UCS} (3.76 GPa), the higher ε_f (4.2%), resulting in the overall increase by 15%, 28% and 45%, compared with these of the (TiC_xN_y–TiB_2)/Ni composites without Al addition.

The strength of the composites is determined by the strength of the reinforcement and matrix, and the interfacial bonding strength between the reinforcements and the matrix. The finer TiC_xN_y and TiB_2 ceramic particles could be the main factor for improving the compression strength and hardness of the (TiC_xN_y–TiB_2)/Ni composites with the Al addition. It has been reported that better reinforcing effect and higher hardness can be achieved in the composites with smaller ceramic particles [13]. On the other hand, the enhanced strength of the matrix is another important factor. As known, the dissolution of Al into Ni can increase the strength of Ni matrix by solid solution strengthening. Due to the increased matrix strength, the compression strength and hardness of the (TiC_xN_y–TiB_2)/Ni composites with the addition of Al is enhanced greatly compared with the (TiC_xN_y–TiB_2)/Ni without the addition of Al. The fracture surfaces of the (TiC_xN_y–TiB_2)/Ni composites with 0 and 5 wt.% Al are shown in Fig. 10. As indicated, in the (TiC_xN_y–TiB_2)/Ni composites without the addition of Al, most of the cracks propagate along the ceramics–matrix interface, while in the composites with the addition of 5 wt.% Al, most of the cracks propagate in the matrix and traverse some of the ceramic particles. It indicates that the matrix strength between the ceramic particles and matrix can be improved by the addition of Al. Table 1 lists the measured density of the (TiC_xN_y–TiB_2)/Ni composites. It can be seen that the measured density of the composites with the addition of Al is lower than that of the composite without the addition of Al, indicating that the excessive addition of Al is not beneficial to the densification of the composites. With the further increasing Al content to 8 wt.%, the relative density of the composites decreases, furthermore, more $AlNi_2Ti$ brittle phase leading to a decline in the compression strength. The enhancement of the strength of the composites with the increase of the Al addition is mainly due to the refinement of the ceramics, the solid solution of Al in the Ni matrix, as well as the improvement of the interfacial bonding strength between the ceramics and the Ni matrix.

4. Conclusions

The 70 vol.% (TiC_xN_y–TiB_2)/Ni composites with 0, 2, 5, 8 wt.% Al were successfully fabricated by the method of combustion synthesis and hot press consolidation in the Ni–Al–Ti–B_4C–BN systems. The addition of Al to Ni–Ti–B_4C–BN system significantly decreased the ignition difficulty, and improved the compression properties of (TiC_xN_y–TiB_2)/Ni composites. With the increase in Al content from 0 to 8 wt.%, the average sizes of the ceramic particles TiC_xN_y and TiB_2 both decrease from 4 to <2 μm due to the decline in the maximum combustion temperature. With the increasing Al content, the hardness and compression strength of the (TiC_xN_y–TiB_2)/Ni composites increase firstly, and then decrease.

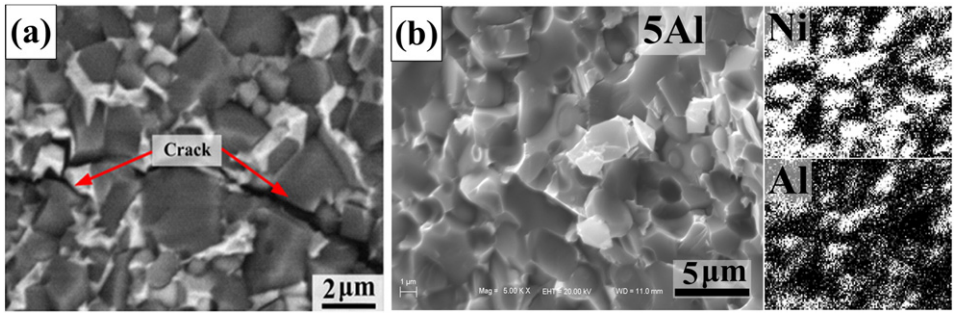

Fig. 10. Fracture surfaces of the (TiC_xN_y–TiB_2)/Ni composites with (a) 0 wt.% and (b) 5 wt.% Al.

The composite with 5 wt.% Al possesses the best comprehensive properties: the highest hardness (1794 Hv), the superior compression strength (3.76 GPa), and the higher fracture strain (4.2%), resulting in an overall increase by 15%, 28% and 45%, compared with these of the (TiC_xN_y–TiB_2)/Ni composites without Al addition, respectively. The enhancement of the strength of the composites with the increase of the Al addition is mainly due to the refinement of the ceramics, the solid solution of Al in the Ni matrix, as well as the improvement of the interfacial bonding strength between the ceramics and the Ni matrix.

Acknowledgments

This work is supported by the National Natural Science Foundation of China (NNSFC, No. 51171071), the National Basic Research Program of China (973 Program, No. 2012CB619600), the NNSFC (No. 51501176), the State Scholarship Fund of China Scholarship Council (201506175140) and the Project 985—High Performance Materials of Jilin University.

References

[1] K. Shobu, T. Watanabe, Y. Enomoto, K. Umeda, Y. Tsuya, Frictional properties of sintered TiN–TiB_2 and Ti(CN)–TiB_2 ceramics at high temperature, J. Am. Ceram. Soc. 70 (1987) C103–C104.
[2] Y.W. Wang, S.L. Shu, F. Qiu, D.S. Zhou, J.G. Wang, Q.C. Jiang, Effect of W content on the compression properties and abrasive wear behavior of the (TiB_2–TiC_xN_y)/(Ni + W) composites, Mater. Des. 45 (2013) 286–291.
[3] Y.F. Yang, Q.C. Jiang, Effect of TiB_2/TiC ratio on the microstructure and mechanical properties of high volume fractions of TiB_2/TiC reinforced Fe matrix composite, Int. J. Refract. Met. Hard Mater. 38 (2013) 137–139.
[4] Z.M. Zhao, L. Zhang, Y.G. Song, W.G. Wang, H.B. Liu, Microstructures and properties of large bulk solidified TiC–TiB_2 composites prepared by combustion synthesis under high gravity, Scr. Mater. 61 (2009) 281–284.
[5] B.V.M. Kumar, B. Basu, Mechanisms of material removal during high temperature fretting of TiCN–Ni based cermets, Int. J. Refract. Met. Hard Mater. 26 (2008) 504–513.
[6] N. Worauaychai, N. Poolthong, R. Tongsri, Reduction of liquid phase formation temperature of TiC–Ni composite by sintering activator addition, Powder Technol. 246 (2013) 478–486.
[7] Y.F. Yang, Q.C. Jiang, A simple route to fabricate TiC–TiB_2/Ni composite via thermal explosion reaction assisted with external pressure in air, Mater. Chem. Phys. 143 (2014) 480–485.
[8] J. Qu, W.H. Xiong, D.M. Ye, Z.H. Yao, W.J. Liu, S.J. Lin, Effect of WC content on the microstructure and mechanical properties of Ti($C_{0.5}N_{0.5}$)–WC–Mo–Ni cermets, Int. J. Refract. Met. Hard Mater. 28 (2010) 243–249.
[9] J. Jung, S. Kang, Effect of ultra-fine powders on the microstructure of Ti(CN)–xWC–Ni cermets, Acta Mater. 52 (2004) 1379–1386.
[10] M. Humenik, N.M. Parikh, Cermets: I, fundamental concepts related to microstructure and physical properties of cermet systems, J. Am. Ceram. Soc. 39 (2) (1956) 60–63.
[11] N.M. Parikh, M. Humenik, Cermets: II, wettability and microstructure studies in liquid-phase sintering, J. Am. Ceram. Soc. 40 (9) (1957) 315–320.
[12] J.C. LaSalvia, D.K. Kim, M.A. Meyers, Effect of Mo on microstructure and mechanical properties of TiC–Ni-based cermets produced by combustion synthesis-impact forging technique, Mater. Sci. Eng. A 206 (1996) 71–80.
[13] S.L. Shu, J.B. Lu, F. Qiu, Q.Q. Xuan, Q.C. Jiang, Effects of alloy elements (Mg, Zn, Sn) on the microstructures and compression properties of high-volume-fraction TiC_x/Al composites, Scr. Mater. 63 (2010) 1209–1211.
[14] H. Boutefnouchet, C. Curfs, A. Triki, A. Boutefnouchet, D. Vrel, Self-propagating high-temperature synthesis mechanisms within the Ti–C–Ni system: a time resolved X-ray diffraction study, Powder Technol. 217 (2012) 443–450.
[15] Y.F. Yang, Q.C. Jiang, Reaction behaviour, microstructure and mechanical properties of TiC–TiB_2/Ni composite fabricated by pressure assisted self-propagating high-temperature synthesis in air and vacuum, Mater. Des. 49 (2013) 123–129.
[16] S.L. Shu, F. Qiu, B. Xing, S.B. Jin, J.G. Wang, Q.C. Jiang, Effect of strain rate on the compression behavior of TiAl and TiAl–2Mn alloys fabricated by combustion synthesis and hot press consolidation, Intermetallics 43 (2013) 24–28.